

See discussions, stats, and author profiles for this publication at: <https://www.researchgate.net/publication/258494758>

Scaling Analysis of Propeller-Driven Aircraft for Mars Exploration

Article in *Journal of Aircraft* · September 2013

DOI: 10.2514/1.C032086

CITATIONS
16

READS
4,967

3 authors:



Tianshu Liu
Western Michigan University
213 PUBLICATIONS 5,552 CITATIONS

[SEE PROFILE](#)



Akira Oyama
Japan Aerospace Exploration Agency
266 PUBLICATIONS 2,545 CITATIONS

[SEE PROFILE](#)



Kozo Fujii
Tokyo University of Science
526 PUBLICATIONS 5,870 CITATIONS

[SEE PROFILE](#)

Scaling Analysis of Propeller-Driven Aircraft for Mars Exploration

Tianshu Liu*

Western Michigan University, Kalamazoo, Michigan 49008

and

Akira Oyama[†] and Kozo Fujii[‡]

Institute of Space and Astronautical Science, Japan Aerospace Exploration Agency,
Sagamihara 252-5210, Japan

DOI: 10.2514/1.C032086

The scaling relations between the performance parameters of propeller-driven aircraft flying on Mars and Earth are discussed, including the cruising velocity, power required for cruising flight, and propulsive power generated by propellers. The power ratio criterion for feasible cruising flight of propeller-driven aircraft on Mars is proposed, and the relevant design parameters are identified. This criterion is first used to examine the feasibility of typical and nontypical aircraft for cruising flight on Mars, and then applied as a guideline to the preliminary design of the sample Martian aircraft. In addition, the constraints on the rotational speed of a propeller in cruising flight on Mars are given, which should be considered in the design of propellers. The methods developed in this paper are also applicable to other space exploration aircraft for Venus and Titan.

Nomenclature

A	= total propeller disk area, $n\pi D_{\text{prop}}^2/4, \text{m}^2$	N	= propeller rotational speed, rev/s
a	= $(4/3)^{1/4}(K/\rho_E^2 C_{D0})^{1/4}$	n	= number of propellers
a_s	= speed of sound, m/s	p_M	= atmospheric pressure on Mars, Pa
AR	= wing aspect ratio	$P_{E,\text{max } R}$	= maximum range power on Earth, W
B	= number of blades	$P_{E,\text{min } P}$	= minimum power on Earth, W
b	= $0.5C_{D0}\rho_E a^3 + 2K/(\rho_E a)$	$P_{M,\text{max } R}$	= maximum range power on Mars, W
c	= mean wing chord or blade chord, m	$P_{M,\text{min } P}$	= minimum power on Mars, W
c_p	= propulsive power coefficient, $c_p = P_{\text{prop}}/(\rho SV^3)$	P_{prop}	= propulsive power, W
C_{D0}	= zero-lift drag coefficient	PIW	= generalized power, W
C_L	= lift coefficient	r	= radial coordinate along blade, m
C_l	= sectional lift coefficient	r_{AS}	= disk-to-wing area ratio, $r_{AS} = A/S$
C_P	= propulsive power coefficient, $C_p = TV/(\rho N^3 D_{\text{prop}}^5)$	r_{motor}	= motor power-to-weight ratio, W/kg
C_T	= thrust coefficient, $C_T = T/\rho N^2 D_{\text{prop}}^4$	R	= propeller radius, m
C_1	= weight coefficient, $C_1 = W_{E,\text{prop}}/A$	Re	= Reynolds number based on mean chord
C_2	= weight coefficient, $C_2 = W_{E,\text{motor}}/P_{\text{prop},E}$	S	= wing area, m ²
C_3	= weight coefficient, $C_3 = (W_{E,\text{wing}} + W_{E,\text{others}})/S$	T	= thrust, N
D_{prop}	= propeller diameter, m	T_M	= atmospheric temperature on Mars, K
e	= Oswald efficiency	UB	= upper bound
g_E	= gravitational constant on Earth, m/s ²	V	= flight velocity, m/s
g_M	= gravitational constant on Mars, m/s ²	$V_{E,\text{max } R}$	= maximum range velocity on Earth, m/s
H	= altitude, km	$V_{E,\text{min } P}$	= minimum-power velocity on Earth, m/s
H_{max}	= maximum cruising altitude on Earth, km	$V_{M,\text{max } R}$	= maximum range velocity on Mars, m/s
J	= advance ratio coefficient, $J = V/ND_{\text{prop}}$	$V_{M,\text{min } P}$	= minimum-power velocity on Mars, m/s
K	= $(\pi A Re)^{-1}$	VIW	= standard airspeed, m/s
K_P	= propulsive power coefficient, $(8/\pi^4)C_P$	W	= weight, N
K_T	= thrust coefficient, $(8/\pi^3)C_T$	W_E	= total weight on Earth, N
M	= Mach number	$W_{E,\text{motor}}$	= motor weight on Earth, N
m_E	= total mass, kg	$W_{E,\text{others}}$	= other weight, N
$m_{E,\text{motor}}$	= motor mass, kg	$W_{E,\text{prop}}$	= propeller weight on Earth, N
$m_{E,\text{others}}$	= other mass, kg	$W_{E,\text{wing}}$	= wing weight on Earth, N
$m_{E,\text{prop}}$	= propeller mass, kg	$W_{E,w-p-m}$	= sum of wing, propeller, and motor weights
$m_{E,\text{wing}}$	= wing mass, kg	x	= normalized radial coordinate, $x = r/R$

Greek

α_S	= empirical constant, $\alpha_S = S/W_E^{2/3}$
β_P	= empirical constant, $\beta_P = P_{\text{prop},E}/W_E^{7/6}$
ϵ	= drag-to-lift ratio
η_{motor}	= motor efficiency
η_{prop}	= propeller efficiency, $\eta_{\text{prop}} = C_T J / C_P$
λ	= advance ratio coefficient, $V/\omega R$
Π_H	= power ratio at H on Earth
Π_M	= power ratio on Mars
ρ	= atmospheric density, kg/m ³
$\rho_{A,\text{prop}}$	= propeller surface density, $\rho_{A,\text{prop}} = W_{E,\text{prop}}/A, \text{kg/m}^2$
ρ_E	= air density on Earth, kg/m ³

Received 28 August 2012; revision received 7 March 2013; accepted for publication 31 March 2013; published online 15 August 2013. Copyright © 2013 by the American Institute of Aeronautics and Astronautics, Inc. All rights reserved. Copies of this paper may be made for personal or internal use, on condition that the copier pay the \$10.00 per-copy fee to the Copyright Clearance Center, Inc., 222 Rosewood Drive, Danvers, MA 01923; include the code 1542-3868/13 and \$10.00 in correspondence with the CCC.

*Professor, Department of Mechanical and Aeronautical Engineering; tianshu.liu@wmich.edu (Corresponding Author). Senior Member AIAA.

[†]Associate Professor, Department of Space Flight Systems; oyama@flab.isas.jaxa.jp. Senior Member AIAA.

[‡]Professor, Department of Space Flight Systems; fujii@flab.isas.jaxa.jp. Fellow AIAA.

ρ_M	=	gas density on Mars, kg/m ³
$\rho_{S,\text{wing}}$	=	wing surface density, $\rho_{S,\text{wing}} = W_{E,\text{wing}}/S$, kg/m ²
σ	=	solidity factor, $\sigma = Bc/\pi R$
ϕ	=	flow angle relative to propeller plane, $\tan^{-1}(\lambda/x)$
ω	=	propeller rotational speed, rad/s

Subscripts

Cri	=	critical value
E	=	Earth
M	=	Mars
Prop	=	propeller
Ref	=	reference
Wing	=	wing

I. Introduction

THE vision of using winged flight vehicles for Mars exploration has been described by von Braun in his book *The Mars Project* [1]. This seemingly remote idea has been seriously considered in several NASA projects, particularly on the Aerial Regional-Scale Environmental Survey (ARES) Mars Scout airplane [2–4]. The scaled ARES Mars airplane prototype has been deployed in high-altitude drop tests. The design of aircraft flying in the Martian thin carbon dioxide atmosphere has encountered some unique problems in aerodynamics, propulsion, and structures [5]. The generation of sufficient lift in such a thin atmosphere is the first challenge, and the immediately related problem is the generation of the sufficient propulsive force. A bipropellant, pulsed-control rocket propulsion system is employed on the ARES Mars airplane as a relatively reliable approach [6]. Recent attention has been focused on solar-powered long-endurance Mars aircraft. Propellers and a flapping wing have been proposed by Colozza [7,8] as propulsion systems for solar-powered Martian aircraft. The preliminary flight performance analysis of solar-powered aircraft has been given by Noth et al. [9,10], Noth and Siegwart [11], and Klesh and Kabamba [12]. The scaling analyses for Martian flight are given by Lorenz [13] and Savu [14]. However, the previous studies fail to provide a clear answer to a fundamental question: whether or not propeller-driven aircraft can cruise on Mars and under what conditions.

The objective of this work is to give a criterion for the feasibility of cruising flight of propeller-driven aircraft on Mars and provide a guideline for the design of such a Martian aircraft. First, the scaling relations are given for propeller-driven aircraft flying on Earth and Mars, which allows the design of Martian aircraft to be based on its counterpart on Earth for convenience. Further scaling analysis leads to a simple criterion of the power ratio that must be stratified for feasible cruising flight on Mars. The power ratio depends on two design parameters: the disk-to-wing area ratio and the propulsive power per unit wing area. The parametric domain for feasible cruising flight on Mars is determined, depending on a set of the design parameters. The power criterion for cruising flight is validated by applying it to typical propeller-driven aircraft on Earth and the Helios Prototype for several interesting predictions. Next, this criterion is applied to the preliminary design of the sample Martian aircraft. Note that the presented analysis can be adapted to the flapping flight on Mars proposed by Colozza [8] because a flapping-wing flyer is similar to propeller-driven aircraft from a standpoint of the momentum stream tube model [15]. Furthermore, the scaling analysis for the performance of propellers of Martian aircraft is conducted. It is found that a much higher rotational speed of the propeller is required on Mars to attain the same propeller efficiency on Earth. On the other hand, the critical rotational speed is given as an upper bound to keep flow on the blade surface subsonic. These conflicting constraints should be considered in the design of propellers for Martian flight.

II. Martian Atmosphere

The Mars environment is different from Earth in several aspects, and therefore the design of a flight vehicle in such an environment encounters some unique challenges. The Martian atmosphere is

made up almost entirely of carbon dioxide. Mars has a very thin atmosphere, and the atmospheric gas density near the surface on Mars is close to the air density at the altitude of 30 km on Earth. As a result, the atmospheric pressure on Mars is considerably lower. The temperature on Mars is on average much lower than on Earth. The gravitational force on Mars is about one-third of that on Earth. Figures 1a–1d show the distributions of the density, pressure, temperature, and speed of sound in the Martian atmosphere, which are approximately linear in the altitude range of 0–10 km. The least-squares regression gives the linear functions of the altitude H (km), i.e., $\rho_M = -5.87 \times 10^{-4}H + 0.0142$ (kg/m³), $p_M = -42.3H + 774.2$ (N/m²), $T_M = -6.22H + 286.8$ (K), and $a_{s,M} = -3.1H + 268.3$ (m/s) in the altitude range of $H = 0$ –10 km, where H is in km. Figure 1e shows the distribution of the dynamic viscosity. The data of the atmospheric density, pressure, temperature, and speed of sound are from the General Mars Atmosphere Model of NASA Langley Research Center (LaRC) and the data of the dynamic viscosity are from the Jet Propulsion Laboratory (JPL), California Institute of Technology Reference Mars Atmosphere for 20° latitude [8].

The important nondimensional parameters in aerodynamics are the Reynolds number and the Mach number. The ratio between the Reynolds numbers at the Martian surface and at sea level on Earth is $Re_M/Re_E = 0.02$ when the flight velocity is the same. Therefore, a Martian flight vehicle must fly in a very low Reynolds number regime and the problems in lift generation and drag due to flow separation at low Reynolds numbers should be considered. The ratio between the Mach numbers at the Martian surface and the sea level on Earth is $M_M/M_E = 1.27$ due to the different speeds of sound. In addition, the ratio between the gravitational accelerations at the Martian surface and the sea level on Earth is $g_M/g_E = 0.383$.

III. Scaling for Fixed-Wing Level Flight

A. Characteristic Velocities and Powers

The objective of this section is to establish the scaling relations of the required velocity and power for fixed-wing flight on Earth and Mars. From an aerodynamic standpoint, the performance of a flight vehicle on Mars is inevitably limited by the very low gas density in the Martian atmosphere. However, the gravitational force on Mars is lower than that on Earth. To take the effects of the gas density and gravity into account, we adapt the PIW–VIW relation in flight testing [16–18]:

$$\text{PIW} = \frac{1}{2} C_{D0} \rho_{\text{ref}} S (\text{VIW})^3 + \frac{2K W_{\text{ref}}^2}{\rho_{\text{ref}} S (\text{VIW})} \quad (1)$$

where the standard airspeed VIW and the generalized power PIW are defined as

$$\text{VIW} = \frac{V(\rho/\rho_{\text{ref}})^{1/2}}{(W/W_{\text{ref}})^{1/2}}, \quad \text{PIW} = \frac{P(\rho/\rho_{\text{ref}})^{1/2}}{(W/W_{\text{ref}})^{3/2}} \quad (2)$$

In flight testing, W and W_{ref} are the weight in the testing condition that typically decreases during flight due to fuel consumption and the standard weight of an aircraft, respectively. The density ratio ρ/ρ_{ref} is introduced to absorb the air density effect at different altitudes, where the reference density ρ_{ref} is typically the air density at sea level. In Eq. (1), the factor $K = (\pi AR e)^{-1}$ is related to the wing aspect ratio AR and the Oswald efficiency e , where C_{D0} is the parasite drag coefficient and S is the projected wing area.

We consider a fixed-wing aircraft with the same geometrical parameters, such as the wing area and wing aspect ratio, on Earth and Mars. The differences in the flight performances of the aircraft on Earth and Mars are mainly determined by the environmental parameters, such as the atmospheric density and the gravity. To compare flight on Earth with that on Mars, W and W_{ref} are substituted by the weight on Mars W_M and weight on Earth W_E of the same aircraft, where the subscripts M and E indicate the conditions on Mars and Earth, respectively. Because the conditions on Earth are considered as the reference conditions, the scaled velocity VIW and the generalized power PIW in Eq. (1) are replaced by the velocity V_E

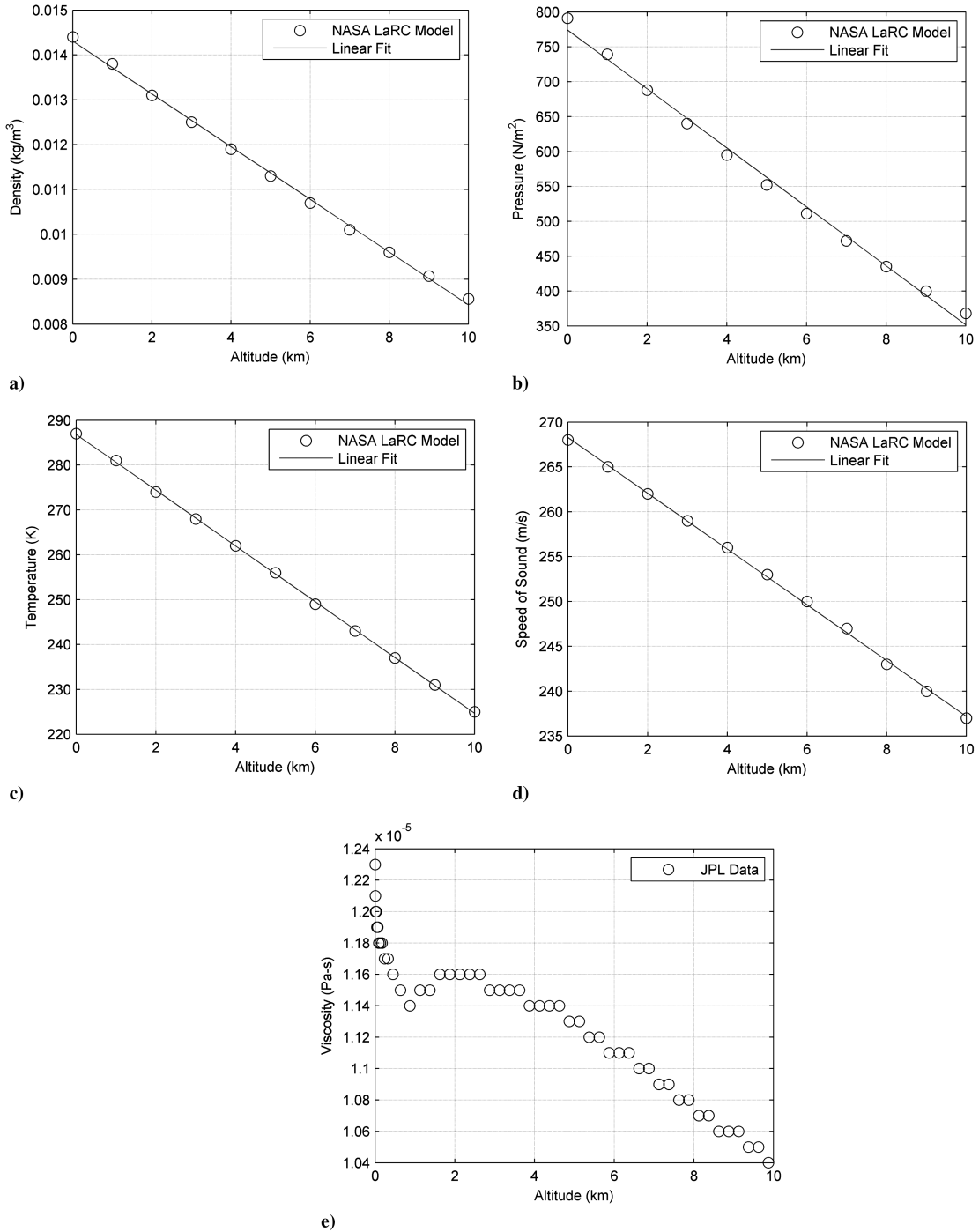


Fig. 1 The atmospheric parameters on Mars for a) density, b) pressure, c) temperature, d) speed of sound, and e) dynamical viscosity.

and power P_E on Earth. Similarly, ρ and ρ_{ref} are replaced by ρ_M and ρ_E , respectively. Therefore, the scaled power–velocity relation is

$$P_E = \frac{1}{2} C_{D0} \rho_E S V_E^3 + \frac{2 K W_E^2}{\rho_E S V_E} \quad (3)$$

where

$$V_E = \frac{V_M (\rho_M / \rho_E)^{1/2}}{(W_M / W_E)^{1/2}}, \quad P_E = \frac{P_M (\rho_M / \rho_E)^{1/2}}{(W_M / W_E)^{3/2}} \quad (4)$$

For simplicity, it is assumed that the aircraft has the same aerodynamic coefficients, such as the lift and drag coefficients and the Oswald efficiency, on Earth and Mars. This assumption is reasonable as the first-order approximation. Otherwise, in general,

C_{D0} and e are replaced by $C_{D0,E} (C_{D0,M} / C_{D0,E})$ and $e_E (e_M / e_E)$, respectively.

Equation (3) determines the level flight performance of an aircraft on Earth [19], and Eq. (4) gives the scaling relations for the velocity and the required power for flight on Earth and Mars. Based on Eq. (3), the velocity at the minimum power on Earth is

$$V_{E,\min P} = a (W_E / S)^{1/2} \quad (5)$$

and the required minimum power at $V_{E,\min P}$ is

$$P_{E,\min P} = b S (W_E / S)^{3/2} \quad (6)$$

where

$$a = (4/3)^{1/4} (K/\rho_E^2 C_{D0})^{1/4} \quad (7)$$

$$b = \frac{1}{2} C_{D0} \rho_E a^3 + \frac{2K}{\rho_E a} = 2 \left(\frac{4}{3} \right)^{3/4} \frac{C_{D0}^{1/4}}{\rho_E^{1/2} (\pi A Re)^{3/4}} \quad (8)$$

According to Eq. (4), the corresponding minimum power and the velocity at the minimum power on Mars for aircraft with the same mass are given by

$$\begin{aligned} V_{M,\min P} &= a \left(\frac{g_M}{g_E} \right)^{1/2} \left(\frac{\rho_E}{\rho_M} \right)^{1/2} \left(\frac{W_E}{S} \right)^{1/2} \\ &= \left(\frac{g_M}{g_E} \right)^{1/2} \left(\frac{\rho_E}{\rho_M} \right)^{1/2} V_{E,\min P} \end{aligned} \quad (9)$$

$$\begin{aligned} P_{M,\min P}/S &= b \left(\frac{g_M}{g_E} \right)^{3/2} \left(\frac{\rho_E}{\rho_M} \right)^{1/2} \left(\frac{W_E}{S} \right)^{3/2} \\ &= \left(\frac{g_M}{g_E} \right)^{3/2} \left(\frac{\rho_E}{\rho_M} \right)^{1/2} P_{E,\min P}/S \end{aligned} \quad (10)$$

where g_E and g_M are the gravitational constants on Earth and Mars, respectively. Equation (9) indicates that $V_{M,\min P}$ of aircraft flying on Mars is proportional to the square root of the wing loading W_E/S , the factor $(g_M/g_E)^{1/2}(\rho_E/\rho_M)^{1/2}$ reflects the effects of the gravity and gas density, and the factor a reflects the effect of the aerodynamic parameters. Similarly, the required power per area $P_{M,\min P}/S$ of an aircraft flying on Mars is proportional to $(W_E/S)^{3/2}$ with the factor $(g_M/g_E)^{3/2}(\rho_E/\rho_M)^{1/2}$ and the factor b . Therefore, the wing loading W_E/S on Earth is considered as the main design parameter. When $\rho_E = 1.225 \text{ kg/m}^3$ at sea level on Earth and $\rho_M = 0.0142 \text{ kg/m}^3$ at the surface on Mars are used, Eqs. (9) and (10) become $V_{M,\min P} = 5.75 V_{E,\min P}$ and $P_{M,\min P} = 2.2 P_{E,\min P}$, where $g_E = 9.8 \text{ m/s}^2$ and $g_M = 3.75 \text{ m/s}^2$. This indicates that a fixed-wing aircraft must fly much faster and use more power on Mars compared to its counterpart on Earth.

Further, the velocity and the required power at the maximum range are proportional to those at the minimum power, i.e., [20]:

$$V_{M,\max R} = 1.35 V_{M,\min P}, \quad P_{M,\max R} = 1.146 P_{M,\min P} \quad (11)$$

Therefore, the scaling relations $V_{M,\max R} = 5.75 V_{E,\max R}$ and $P_{M,\max R} = 2.2 P_{E,\max R}$ hold on the sea level on Earth and the surface of Mars. According to Liu [20], typical propeller-driven aircraft on Earth follow a set of the scaling laws, listed in Table 1. For such typical aircraft with $C_{D0} = 0.03$, $AR = 8.15$, and $e = 0.75$, Fig. 2 shows the cruising velocity $V_{M,\max R}$ and the required power per wing area $P_{M,\max R}/S$ on Mars as a function of the wing loading W_E/S . The lift coefficients on Earth and Mars have the scaling relation

$$C_{L,M} = \left(\frac{g_M}{g_E} \right) \left(\frac{\rho_E}{\rho_M} \right) \left(\frac{V_E}{V_M} \right)^2 C_{L,E} \quad (12)$$

Interestingly, by substituting the velocity scaling relations Eqs. (9) and (11) into Eq. (12), it is found that the lift coefficient of the same aircraft in cruising flight on Earth and Mars remains invariant, i.e., $C_{L,M} = C_{L,E}$.

The thrust generated by propellers is given by $T = n C_T \rho N^2 D_{prop}^4 = n C_T \rho D_{prop}^2 V^2 / J^2$, where C_T is the thrust coefficient, V is the incoming velocity, N is the angular propeller speed (rev/s), D_{prop} is the diameter of a propeller, n is the number of propellers, and $J = V/N D_{prop}$ is the advance ratio coefficient. The power coefficient and the propeller efficiency are defined as $C_P = TV/(\rho N^3 D_{prop}^5)$ and $\eta_{prop} = C_T J / C_P$, respectively [21]. By introducing the total propeller disk area $A = n \pi D_{prop}^2 / 4$ and the ratio between the disk area and the wing area $r_{AS} = A/S$, the propulsive power provided by a propeller is given by

Table 1 Scaling laws and derived results for propeller aircraft on Earth

Quantity	Scaling law
Upper limit or max TO weight	$W_{MTO} = 1.282 \text{ W}$
Wingspan	$b_{wing} = 0.462 \text{ W}^{1/3}$
Wing area	$S_{wing} = 0.0262 \text{ W}^{2/3}$
Mean chord	$c = 0.0567 \text{ W}^{1/3}$
Aspect ratio	8.15
Body length	$l_{body} = 0.41 \text{ W}^{1/3}$
Max body diameter	$d_0 = 0.0481 \text{ W}^{1/3}$
Wet and wing area ratio	4.35
Body fineness ratio	8.52
Wing loading	$WL = 53 \text{ W}^{1/3}$
Reynolds number	$Re_c = 6.2 \times 10^4 \text{ W}^{1/2}$
Cruise speed	$V_{max R} = 15.52 \text{ W}^{1/6}$
Cruise power	$P_{max R,aircraft} = 1.67 \text{ W}^{7/6}$
Power available	$P_{prop} = 5.25 \text{ W}^{1.13}$
Engine weight	$W_{engine} = 0.327 \text{ W}^{0.8944}$
Max L/D	11.9
Oswald efficiency	$e = 0.6-0.9$
Parasite drag	$C_{D_{para},S_{wing}} = 0.02-0.044$
Induced drag	$C_{D_{in},S_{wing}} = 0.0032/e$
Propulsive efficiency	$\eta_{prop} = 29.32 \rho C_{D,S_{wing}}$

Note: Units: N for weight, m for length, m^2 for area, m/s for velocity, W for power, kg/m^3 for density, and N/m² for loading.

The mean relative errors associated with the scaling laws are indicated by Liu [20].

$$P_{prop} = \eta_{prop} \left(\frac{4C_P}{\pi J^3} \right) \rho r_{AS} S V^3 = c_P \rho S V^3 \quad (13)$$

where $c_P = P_{prop}/(\rho S V^3) = \eta_{prop} r_{AS} (4C_P/\pi J^3)$ is another power coefficient that is introduced for convenient use in some cases. For

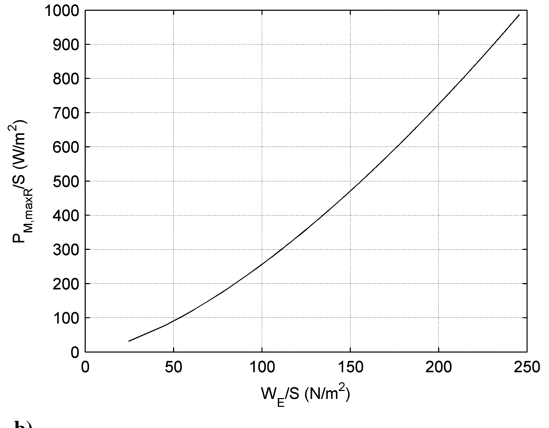
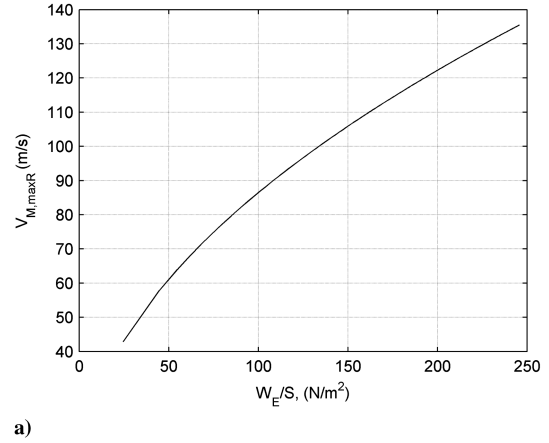


Fig. 2 a) The cruising velocity $V_{M,\max R}$ and b) the required power per wing area $P_{M,\max R}/S$ on Mars as a function of the wing loading W_E/S .

propeller-driven fixed-wing aircraft flying at the same velocity on Earth and Mars, the scaling relation for the propulsive power generated by propellers is

$$\frac{P_{\text{prop},M}}{P_{\text{prop},E}} = \left(\frac{c_{P,M}}{c_{P,E}} \right) \left(\frac{\rho_M}{\rho_E} \right) \quad (14)$$

When the gas densities at the sea level on Earth and the surface on Mars are used, Eq. (14) becomes $P_{\text{prop},M} = 0.0116(c_{P,M}/c_{P,E})P_{\text{prop},E}$.

B. Power Criterion for Cruising Flight on Mars

The criterion for cruising flight of propeller-driven aircraft on Mars can be obtained by substituting the scaling law $P_{\text{prop},E} = \beta_P W_E^{7/6}$ for propeller-driven aircraft on Earth into Eq. (14), where the corresponding propulsive power on Mars is given by

$$P_{\text{prop},M} = \beta_P \left(\frac{c_{P,M}}{c_{P,E}} \right) \left(\frac{\rho_M}{\rho_E} \right) W_E^{7/6} \quad (15)$$

On the other hand, by using a scaling law $S = \alpha_S W_E^{2/3}$ for the wing area and Eqs. (7), (10), and (11), the power required for cruising flight on Mars can be expressed as

$$P_{M,\text{max } R} = \frac{1.146b}{\alpha_S^{1/2}} \left(\frac{g_M}{g_E} \right)^{3/2} \left(\frac{\rho_E}{\rho_M} \right)^{1/2} W_E^{7/6} \quad (16)$$

The coefficients α_S and β_P are the design parameters. Using least-squares fit to the data for a large number of propeller/turboprop aircraft on Earth, Liu [20] gave $\alpha_S = 0.0262$ and $\beta_P = 5.25$ for typical propeller-driven aircraft on Earth. Note that the empirical scaling law given by Liu [20] is $P_{\text{prop},E} = 5.25W_E^{1.13}$, where the empirical exponent of 1.13 is very close to the theoretical value of 7/6 with a relative error of 3%.

For sustainable cruising flight on Mars, the criterion $P_{\text{prop},M}/P_{M,\text{max } R} \geq 1$ must be satisfied, which leads to

$$\Pi_M \equiv \frac{P_{\text{prop},M}}{P_{M,\text{max } R}} = 0.873 \frac{\alpha_S^{1/2} \beta_P}{b} \left(\frac{c_{P,M}}{c_{P,E}} \right) \left(\frac{g_E}{g_M} \right)^{3/2} \left(\frac{\rho_M}{\rho_E} \right)^{3/2} \geq 1 \quad (17)$$

Here, the power ratio Π_M is introduced for propeller-driven Martian aircraft. In particular, when the conditions at the sea level on Earth and the surface on Mars are used, the power criterion Eq. (17) becomes

$$\Pi_M = 4.6 \times 10^{-3} \frac{\alpha_S^{1/2} \beta_P}{b} \left(\frac{c_{P,M}}{c_{P,E}} \right) \geq 1 \quad (18)$$

The ratio between the power coefficients on Mars and Earth in Eq. (18) can be expressed as

$$\frac{c_{P,M}}{c_{P,E}} = \frac{A/S}{(A/S)_E} \frac{(\eta_{\text{prop}} C_p J^{-3})_M}{(\eta_{\text{prop}} C_p J^{-3})_E} \quad (19)$$

where $(A/S)_E$ is the reference disk-to-wing area ratio of typical propeller-driven aircraft on Earth. The power criterion Eq. (17) can be used not only to examine the feasibility of existing fixed-wing aircraft for Martian flight, but also to provide a guideline to design a feasible Martian aircraft.

For propeller-driven aircraft, the total weight is decomposed into

$$W_E = W_{E,\text{wing}} + W_{E,\text{prop}} + W_{E,\text{motor}} + W_{E,\text{others}} \quad (20)$$

where $W_{E,\text{wing}}$, $W_{E,\text{prop}}$, and $W_{E,\text{motor}}$ are the wing, propeller, and motor weights, respectively, and $W_{E,\text{others}}$ is the weight of the remaining parts, including control and communication units. As a weight constraint, Eq. (20) can be written as

$$\frac{W_E}{S} = C_1 \left(\frac{A}{S} \right) + C_2 \left(\frac{P_{\text{prop},E}}{S} \right) + C_3 \quad (21)$$

where the weight coefficients are

$$\begin{aligned} C_1 &= W_{E,\text{prop}}/A & C_2 &= W_{E,\text{motor}}/P_{\text{prop},E} \\ C_3 &= (W_{E,\text{wing}} + W_{E,\text{others}})/S \end{aligned} \quad (22)$$

that represent the relative contributions to the wing loading from the propellers, motors, and wing plus other parts, respectively. Further, substitution of $\beta_P = P_{\text{prop},E} W_E^{-7/6}$ and $\alpha_S = SW_E^{-2/3}$ into Eq. (18) yields another form:

$$\Pi_M = C_4 \left(\frac{A}{S} \right) \left(\frac{W_E}{S} \right)^{-3/2} \left(\frac{P_{\text{prop},E}}{S} \right) \geq 1 \quad (23)$$

where the proportional coefficient is

$$C_4 = \frac{4.6 \times 10^{-3}}{b(A/S)_E} \frac{(\eta_{\text{prop}} C_p J^{-3})_M}{(\eta_{\text{prop}} C_p J^{-3})_E} \quad (24)$$

By substituting Eq. (21) into Eq. (23) and using the simple notations

$$x_1 = A/S, \quad x_2 = P_{\text{prop},E}/S \quad (25)$$

the power ratio Π_M can be expressed as a function of only the two variables, i.e.,

$$\Pi_M = C_4 \frac{x_1 x_2}{(C_1 x_1 + C_2 x_2 + C_3)^{3/2}} \geq 1 \quad (26)$$

The main design parameters in Eq. (26) are the disk-to-wing area ratio $x_1 = A/S$ and the propulsive power per unit wing area $x_2 = P_{\text{prop},E}/S$. The wing loading is given by a linear function $W_E/S = C_1 x_1 + C_2 x_2 + C_3$. Geometrically, the function $\Pi_M(x_1, x_2)$ gives a surface of the power ratio that intersects with the plane $\Pi_M = 1$. The parametric domain in which the criterion $\Pi_M \geq 1$ is satisfied is demarcated by an intersecting curve

$$C_4 x_1 x_2 - (C_1 x_1 + C_2 x_2 + C_3)^{3/2} = 0$$

Because the propulsive power can be expressed in $P_{\text{prop},E} = g_E r_{\text{motor}} \eta_{\text{prop},E} W_{E,\text{motor}}$, we know $C_2 = W_{E,\text{motor}}/P_{\text{prop},E} = g_E (r_{\text{motor}} \eta_{\text{prop},E})^{-1}$, where r_{motor} is the power-to-weight ratio of a motor in W/kg and $\eta_{\text{prop},E}$ is the propeller efficiency on Earth. Therefore, to explicitly elucidate the effects of the relevant parameters on the power ratio Π_M , Eq. (26) can be expressed as

$$\Pi_M = C_5 \frac{(ARe)^{3/4}}{C_{D0}^{1/4}} (r_{\text{motor}} \eta_{\text{prop},E})^{3/2} \left(\frac{\eta_{\text{prop},M}}{\eta_{\text{prop},E}} \right) f(x_1, x_2) \geq 1 \quad (27)$$

where

$$C_5 = 1.45 \times 10^{-4} \frac{\rho_E^{1/2}}{(A/S)_E} \frac{(C_p J^{-3})_M}{(C_p J^{-3})_E} \quad (28)$$

$$f(x_1, x_2) = \frac{x_1 x_2}{[(C_1/C_2)x_1 + x_2 + C_3/C_2]^{3/2}} \quad (29)$$

According to Eq. (27), the power-to-weight ratio r_{motor} of a motor and the propeller efficiency $\eta_{\text{prop},E}$ on Earth have the major impacts on Π_M because their power-law exponent is 3/2. The wing aspect ratio AR and the Oswald efficiency e also have significant effects because their power-law exponent is 3/4. The effect of the zero-lift drag coefficient C_{D0} is relatively weak due to the smaller power-law exponent of -1/4.

Further, because the lift coefficient in cruising flight can be written as $C_{L,E} = 2W_E/\rho_E V_{E,\max R}^2 S = 0.95(C_{D0}\pi AR)^{1/2}$, Eq. (27) can be recasted in

$$\Pi_M = C_6 \left(\frac{C_{L,E}^{3/2}}{C_{D0}} \right) (r_{\text{motor}} \eta_{\text{prop},E})^{3/2} \left(\frac{\eta_{\text{prop},M}}{\eta_{\text{prop},E}} \right) f(x_1, x_2) \geq 1 \quad (30)$$

where

$$C_6 = 6.63 \times 10^{-5} \frac{\rho_E^{1/2}}{(A/S)_E} \frac{(C_P J^{-3})_M}{(C_P J^{-3})_E} \quad (31)$$

From an aerodynamic point of view, Eq. (30) is more interesting because the factor $C_{L,E}^{3/2}/C_{D0}$ resembles the factor $C_L^{3/2}/C_D$ in the required power and the endurance equation for fixed-wing aircraft, except that C_{D0} is used rather than C_D [19]. The coefficients C_4 , C_5 , and C_6 are related to $\eta_{\text{prop},M}/\eta_{\text{prop},E}$ and $C_{P,M}/C_{P,E}$. As indicated in Sec. VI., when the advance ratio coefficient remains the same on Mars and Earth (i.e., $J_M/J_E = 1$), $\eta_{\text{prop},M}/\eta_{\text{prop},E} = 1$ and $C_{P,M}/C_{P,E} = 1$. In this case, all the terms related to C_P and J in the preceding equations are factored out.

C. Reduced Case on Earth

When ρ_E and ρ_M are replaced by the air density ρ_{SL} at the sea level and the air density $\rho(H)$ at the altitude H on Earth, respectively, Eq. (17) can be reduced to the criterion for cruising flight at the altitude H on Earth, i.e.,

$$\Pi_H \equiv 0.873 \frac{\alpha_S^{1/2} \beta_P}{b} \left(\frac{c_{P,H}}{c_{P,\text{SL}}} \right) \left(\frac{\rho(H)}{\rho_{\text{SL}}} \right)^{3/2} \geq 1 \quad (32)$$

For convenience, Π_H is called the power ratio for propeller-driven aircraft at the altitude H . Accordingly, Eq. (26) can be expressed as

$$\Pi_H = C_{4,E} \frac{x_1 x_2}{(C_1 x_1 + C_2 x_2 + C_3)^{3/2}} \geq 1 \quad (33)$$

where

$$C_{4,E} = \frac{0.873}{b(A/S)_{\text{SL}}} \frac{(\eta_{\text{prop}} C_P J^{-3})_H}{(\eta_{\text{prop}} C_P J^{-3})_{\text{SL}}} \left(\frac{\rho(H)}{\rho_{\text{SL}}} \right)^{3/2} \quad (34)$$

Applications of Eqs. (32) and (33) are discussed in Sec. IV.

D. Upper Bound of Total Weight

From Eq. (23), the upper bound UB of the total weight for cruising flight on Mars can be estimated by setting $\Pi_M = 1$, i.e.,

$$\text{UB}(W_E) = C_4^{2/3} A^{2/3} P_{\text{prop},E}^{2/3} S^{-1/3} \quad (35)$$

Equation (35) indicates that the upper bound $\text{UB}(W_E)$ is mainly determined by A , $P_{\text{prop},E}$, and S . The propulsive power is given by $P_{\text{prop},E} = g_E r_{\text{motor}} \eta_{\text{prop},E} W_{E,\text{motor}}$. The wing area and propeller disk area can be given by $S = W_{E,\text{wing}}/\rho_{S,\text{wing}}$ and $A = W_{E,\text{prop}}/\rho_{A,\text{prop}}$, where $\rho_{S,\text{wing}}$ is the surface density of a wing over the wing area S and $\rho_{A,\text{prop}}$ is the surface density of a propeller over the disk area A . Therefore, Eq. (35) can be expressed as a relation between the weights, i.e.,

$$\text{UB}(W_E) = B_1 W_{E,\text{motor}}^{2/3} W_{E,\text{prop}}^{2/3} W_{E,\text{wing}}^{-1/3} \quad (36)$$

where

$$B_1 = C_4^{2/3} (g_E r_{\text{motor}} \eta_{\text{prop},E})^{2/3} \rho_{A,\text{prop}}^{-2/3} \rho_{S,\text{wing}}^{1/3} \quad (37)$$

By using the weight constraint $W_{E,w-p-m} = W_{E,\text{wing}} + W_{E,\text{prop}} + W_{E,\text{motor}}$ and the following notations

$$y_1 = W_{E,\text{motor}}/W_{E,w-p-m}, \quad y_2 = W_{E,\text{wing}}/W_{E,w-p-m} \quad (38)$$

Equation (36) can be written as

$$\text{UB}(W_E) = B_1 W_{E,w-p-m} g(y_1, y_2) \quad (39)$$

where $g(y_1, y_2) = y_1^{2/3} y_2^{-1/3} (1 - y_1 - y_2)^{2/3}$ is referred to as the weight function. Clearly, the condition imposed on y_1 and y_2 is $y_1 + y_2 < 1$. The relative propeller weight is given by a linear function $W_{E,\text{prop}}/W_{E,w-p-m} = 1 - y_1 - y_2$.

Figure 3a shows the weight function $g(y_1, y_2)$. Interestingly, there are the local maxima in $y_1 = W_{E,\text{motor}}/W_{E,w-p-m}$ that are marked on the surface. However, there is no maxima in $y_2 = W_{E,\text{wing}}/W_{E,w-p-m}$. The location of the local maxima in the plane (y_1, y_2) is plotted in Fig. 3b. The typical cross-sectional profiles of $g(y_1, y_2)$ in $y_1 = W_{E,\text{motor}}/W_{E,w-p-m}$ are shown in Fig. 3c at three values of $y_2 = W_{E,\text{wing}}/W_{E,w-p-m}$, indicating the change of the maxima. It is noted that the theoretical maxima may not be achieved practically due to the limitations of the weights of motors and materials of wing and blades. However, because most portions of the surface of $g(y_1, y_2)$ are relatively flat, the seasonable selection of $W_{E,\text{motor}}/W_{E,w-p-m}$ and $W_{E,\text{wing}}/W_{E,w-p-m}$ could be made.

IV. Application and Validation of Power Criterion

A. Typical Propeller-Driven Aircraft

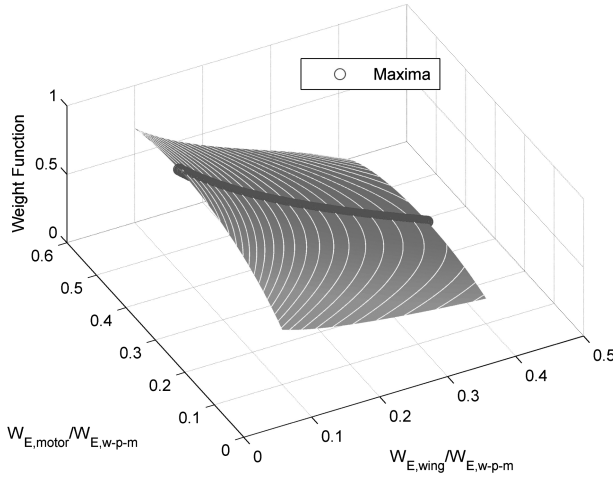
The power ratio criterion is applied to existing aircraft for not only the validation of the criterion itself, but also for the critical examination of their feasibility for flight on Mars. We consider typical propeller-driven aircraft on Earth that is a statistical representation of a large class of propeller-driven aircraft. The scaling laws for the wing area, the propulsive power available, and the cruising velocity are $S = \alpha_S W_E^{2/3}$, $P_{\text{prop},E} = \beta_P W_E^{7/6}$, and $V_{\max R} = 15.52 W_E^{1/6}$, respectively, where $\alpha_S = 0.0262$ and $\beta_P = 5.25$ [20]. The relevant parameters are $C_{D0} = 0.03$, $AR = 8.15$, $e = 0.75$, and $b = 0.1$.

First, the ratio between the propeller disk area and the wing area is estimated. By using the preceding scaling laws, the propulsive power in cruising flight can be also written as $P_{\text{prop},E} = c_P \rho S V_{\max R}^3 = 3.74 \times 10^{-3} c_P \rho \alpha_S W_E^{7/6}$, and therefore an estimate of the power coefficient is $c_P = 2.68 \times 10^{-4} (\beta_P/\alpha_S) \rho^{-1}$. Based on the definition $c_P = \eta_{\text{prop}} r_{AS} (4C_P/\pi J^3)$, we have an estimate of the disk-to-wing area ratio for typical propeller-driven aircraft:

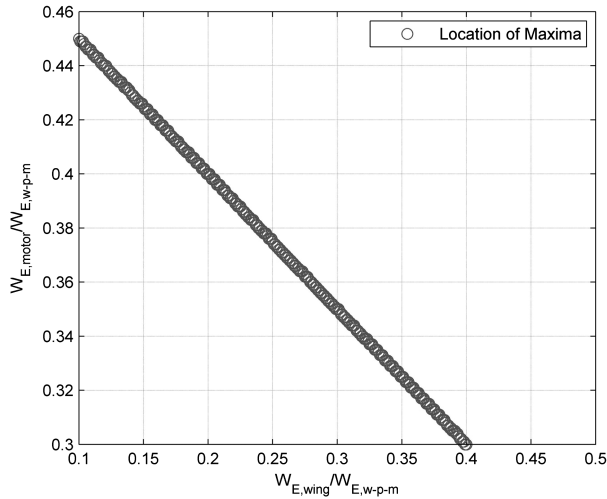
$$r_{AS} = A/S = 2.68 \times 10^{-4} \left(\frac{\beta_P}{\alpha_S} \right) \left(\frac{1}{\rho \eta_{\text{prop}}} \right) \left(\frac{\pi J^3}{4C_P} \right) \quad (40)$$

For a typical propeller that reaches the maximum propulsive efficiency $\eta_{\text{prop}} = 0.7$ at $J = 0.6$, the corresponding power coefficient is $C_P = 0.07$ [22,23]. The disk-to-wing area ratio r_{AS} is inversely proportional to the atmospheric density at cruising altitude, and thus, r_{AS} should increase with the cruising altitude. At the sea level on Earth where $\rho_{\text{SL}} = 1.225 \text{ kg/m}^3$, Eq. (40) gives a lower bound estimate of the disk-to-wing area ratio $r_{AS} = A/S = 0.18$. Figure 4 shows the disk-to-wing area ratio for propeller-driven aircraft compared to the low bound estimate of $r_{AS} = 0.18$. The data are collected from *Jane's All the World's Aircraft 2011–2012* [24]. Single-propeller aircraft usually flying below the altitude of 5 km have an approximate disk-to-wing area ratio of $r_{AS} = 0.2$, which is slightly higher than the estimated low bound. For two- and four-propeller aircraft that have cruising altitudes of 5–10 km, the estimated disk-to-wing area ratio is $r_{AS} = 0.3–0.5$, which approximately agrees with the data of the existing aircraft.

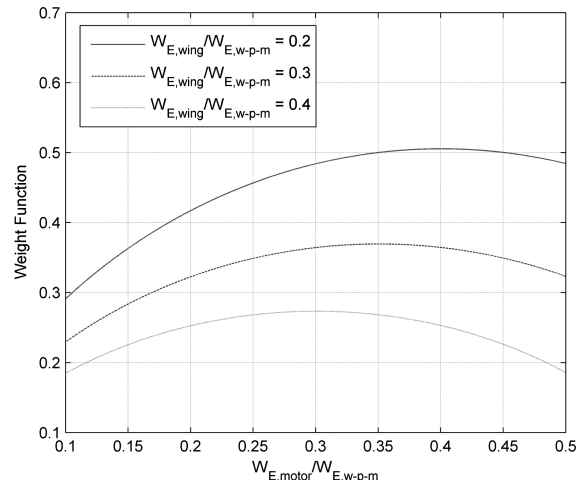
Another interesting application of the power ratio criterion is the determination of the upper flight ceiling of typical propeller-driven aircraft by setting $\Pi_H = 1$ in Eq. (32). For typical propeller-driven aircraft, when the performance of propellers remains the same on the sea level and the altitude H as indicated in Sec. VI (i.e., $c_{P,H} = c_{P,\text{SL}}$), the condition of $\Pi_H = 1$ gives the density ratio $\rho(H_{\max})/\rho_{\text{SL}} = 1.095 b^{2/3} \alpha_S^{-1/3} \beta_P^{-2/3} = 0.263$, and therefore the



a)



b)



c)

Fig. 3 a) Surface of $g(y_1, y_2)$ marked with the maxima, b) the location of the maxima in (y_1, y_2) , and c) cross-sectional profiles of $g(y_1, y_2)$.

maximum cruising altitude is $H_{\max} = 11.9$ km. Figure 5 shows the maximum altitudes of the existing propeller-driven aircraft compared to the estimated cruising flight ceiling of typical propeller-driven aircraft. The service ceiling of propeller-driven aircraft approaches this estimated value as the weight increases. A few nontypical high-altitude aircraft like the Helios Prototype have higher service ceilings.

Further, the surface of Π_H is generated as a function of $x_1 = A/S$ and $x_2 = P_{\text{prop},E}/S$. For typical propeller-driven aircraft,

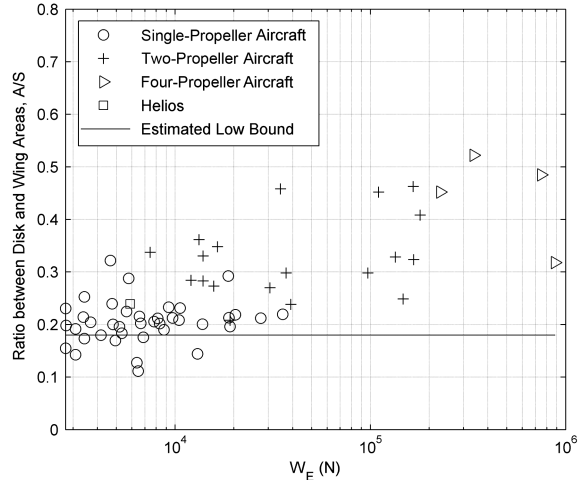


Fig. 4 The disk-to-wing area ratio of propeller-driven aircraft compared to the estimated low bound.

$W_{E,\text{others}} = W_{\text{MTO}} - W_E = 0.786W_E$, where $W_{\text{MTO}} = 1.786W_E$ is the maximum takeoff weight [20]. Because $S = 0.0262W_E^{2/3}$, a scaling law is $W_{E,\text{others}}/S = 30W_E^{1/3}$. Figure 6a shows the Π_H surface for single-propeller aircraft of 300 kg. The intersection between the surface $\Pi_H(x_1, x_2)$ and the plane $\Pi_H(x_1, x_2) = 1$ demarcates the low bound boundary of the cruising flight domain for single-propeller aircraft, which is given by $C_4x_1x_2 - (C_1x_1 + C_2x_2 + C_3)^{3/2} = 0$. The data for single-propeller aircraft of 300–3600 kg are plotted in Fig. 6a for comparison, which are within the demarcated domain for cruising flight as expected. The corresponding plot for two-propeller aircraft of 1500–18,000 kg is given in Fig. 6b, where the low bound boundary is given for an aircraft of 1500 kg.

The preceding results for propeller-driven aircraft on Earth validate the applicability of the power ratio criterion. A more relevant problem is whether or not typical propeller-driven aircraft on Earth can fly on Mars. When the performance of propellers remains the same on Earth and Mars, the power ratio is $\Pi_M = 0.039 < 1$, and therefore typical propeller-driven aircraft on Earth cannot fly on Mars. A feasible Martian aircraft must be nontypical in sizing, weight distribution, and power requirements.

B. Helios Prototype

The Helios Prototype is a nontypical aircraft on Earth [25]. It is a solar-powered high-altitude flying wing aircraft that has a wingspan of 75.3 m, a wing chord of 2.44 m (the total wing area is 184 m²) and the empty weight of 600 kg. Its propulsion system consists of 14 2-m-diam propellers driven by 14 DC electrical motors rated at 1.5 kW.

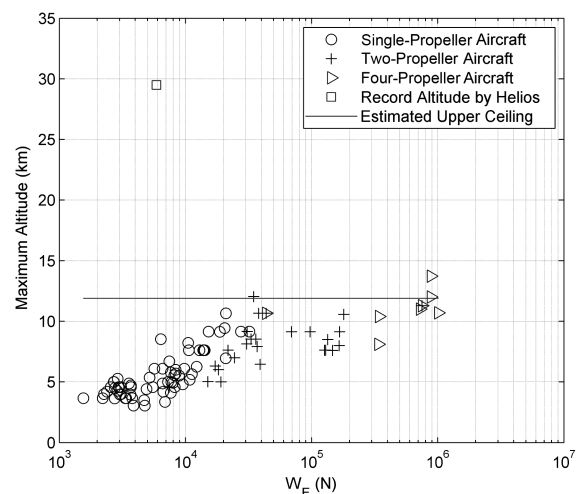


Fig. 5 The maximum altitude of propeller-driven aircraft compared to the estimated upper ceiling for cruising flight.

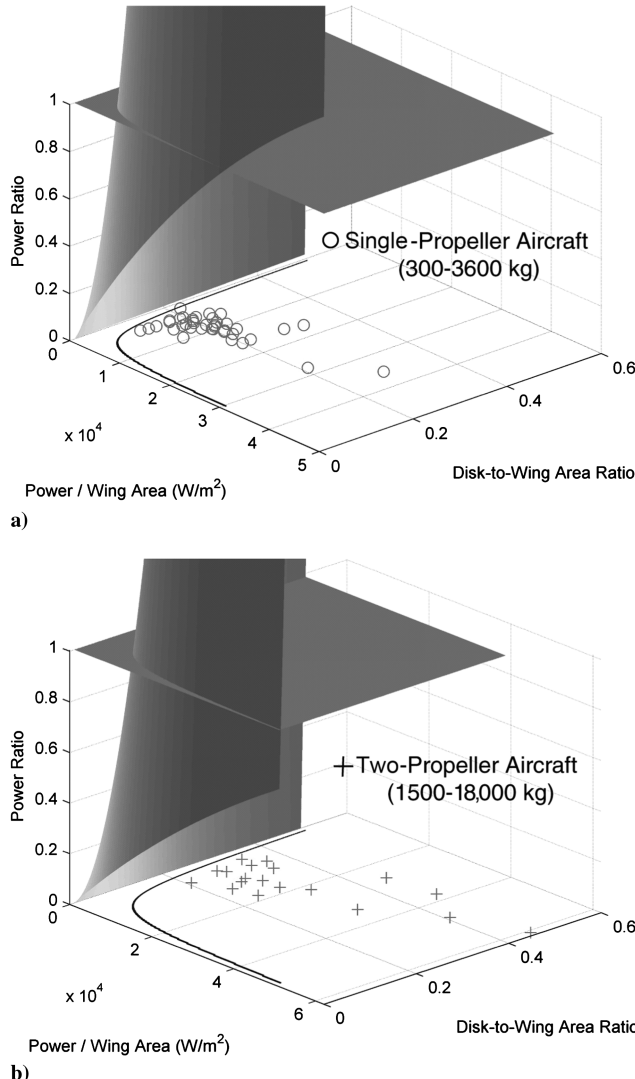


Fig. 6 Typical surface of the power ratio Π_H intersecting with the plane $\Pi_H = 1$ for a) a single-propeller aircraft and b) a two-propeller aircraft.

Solar cells cover upper wing surfaces. Although the Helios Prototype reached the record altitude of 29.5 km, its typical cruising altitude is in 15–21 km. Table 2 lists the relevant parameters of the Helios Prototype compared to those of the typical propeller-driven aircraft and the sample Martian aircraft. For the Helios, $\alpha_S = S/W_E^{2/3} = 0.564$ is much larger than $\alpha_S = 0.0262$ for a typical aircraft, indicating that its wing area is unusually large relative to its weight as an ultralight aircraft. However, $\beta_P = P_{\text{prop},E}/W_E^{7/6} = 0.67$ for the Helios is much smaller than $\beta_P = 5.25$ for typical propeller-driven aircraft, indicating that it is considerably underpowered. The disk-to-wing area ratio $r_{AS} = A/S = 0.24$ of the Helios is close to that for typical single-propeller aircraft. Because of the very large wing aspect ratio AR = 30.9 of the Helios, the parameter $b = 0.025$ defined in Eq. (8) for the Helios is much smaller than $b = 0.1$ for typical propeller-driven aircraft. Based on the preceding parameters

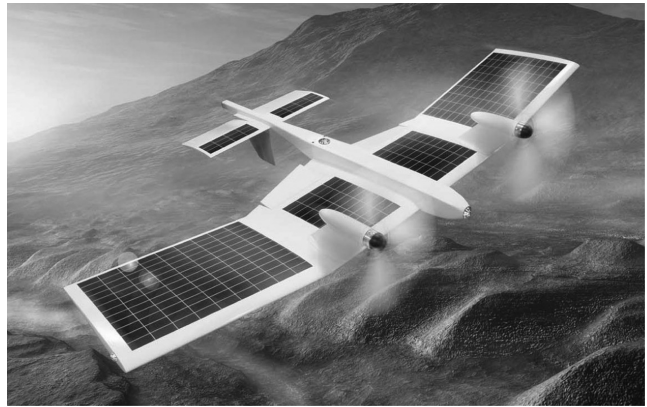


Fig. 7 Sample Martian aircraft model of the Japan Aerospace Exploration Agency.

of the Helios, the estimated maximum cruising altitude is 16.1 km, which is near the lower bound of the Helios' typical cruising altitude range from 15–21 km (NASA Dryden Fact Sheet⁸). However, the power ratio is $\Pi_M = 0.12 < 1$ for the Helios, and therefore even the Helios cannot do sustainable flight on Mars.

V. Sample Martian Aircraft of the Japan Aerospace Exploration Agency

The preliminary design of a solar-powered Martian aircraft of the Japan Aerospace Exploration Agency has been made as an optimization problem by using an evolutional algorithm [26]. The Japan Aerospace Exploration Agency Martian aircraft is considered as a sample Martian aircraft. Figure 7 is an illustration of the sample Martian aircraft model with two propellers. Note that the sample Martian aircraft in this design has four propellers. Table 3 lists the basic geometric parameters of this aircraft. Table 4 shows the assumed parameters evaluate the power ratio and the performance parameters of this aircraft. The procedures of estimating the performance parameters are given in the following steps.

1) The total weight W_E in the initial design is assigned as the upper bound, i.e., $W_E \rightarrow \text{UB}(W_E)$. Then, by using Eq. (35), the minimum required propulsive power $P_{\text{prop},E}$ on Earth and the corresponding minimum motor power P_{motor} are estimated for the given design parameters in Table 3. The upper bound of the total weight of the sample Martian aircraft is shown in Fig. 8, where the propulsive power $P_{\text{prop},M}$ on Mars and the total weight of the aircraft in the design is marked. The design point is below the upper bound.

2) The weights of the motor, wing, and propeller are estimated when the motor power-to-weight ratio, wing surface density, propeller material density, propeller solidity, and mean propeller thickness are given.

3) The Martian power ratio Π_M is calculated as a function of $x_1 = A/S$ and $x_2 = P_{\text{prop},M}/S$. Figure 9a shows the surface of Π_M intersecting with the plane $\Pi_M = 1$. As shown in Fig. 9a, the design point at which $\Pi_M = 1.44 > 1$ is within the boundary given by $C_4x_1x_2 - (C_1x_1 + C_2x_2 + C_3)^{3/2} = 0$ demarcating the parametric domain in the plane (x_1, x_2) for feasible Martian flight. Then, the wing loading is calculated by using $W_E/S = x_3 = C_1x_1 + C_2x_2 + C_3$. Figure 9b shows the wing loading plane on Earth for the sample Martian aircraft.

4) When the wing loading W_E/S is given, the velocity, power, and lift coefficient required for cruising on Earth and Mars are estimated.

5) The cruising range and endurance are estimated when the energy density and weight of the batteries are given.

6) The criterion $\Pi_M \geq 1$ for cruising flight on Mars in the initial design is examined. If $\Pi_M < 1$, the initial design parameters should be adjusted. According to Eq. (23), the major parameters are the disk-to-wing area ratio A/S , the propulsive power per unit wing area

⁸Data available online at <http://www.nasa.gov/centers/dryden/news/FactSheets/FS-068-DFRC.html> [retrieved 1 December 2009].

Table 2 Parameters of several propeller-driven aircraft

Parameters	α_S	β_P	A/S	b	Cruise H_{\max}	Π_M
Typical aircraft	0.0262	5.25	0.18	0.1	11.8 km	0.039
Helios	0.564	0.67	0.24	0.025	16.1 km	0.12
Canyon flyer	0.023	0.97	1.2	0.1	—	0.042
Sample Martian aircraft of Japan Aerospace Exploration Agency	0.096	23.3	1.1	0.12	20.4 km	1.44

Table 3 Basic geometric parameters of sample propeller-driven Martian aircraft

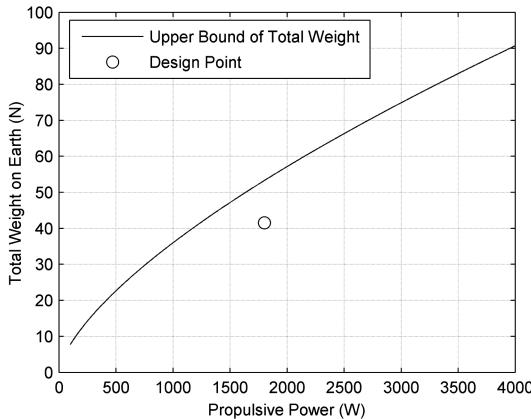
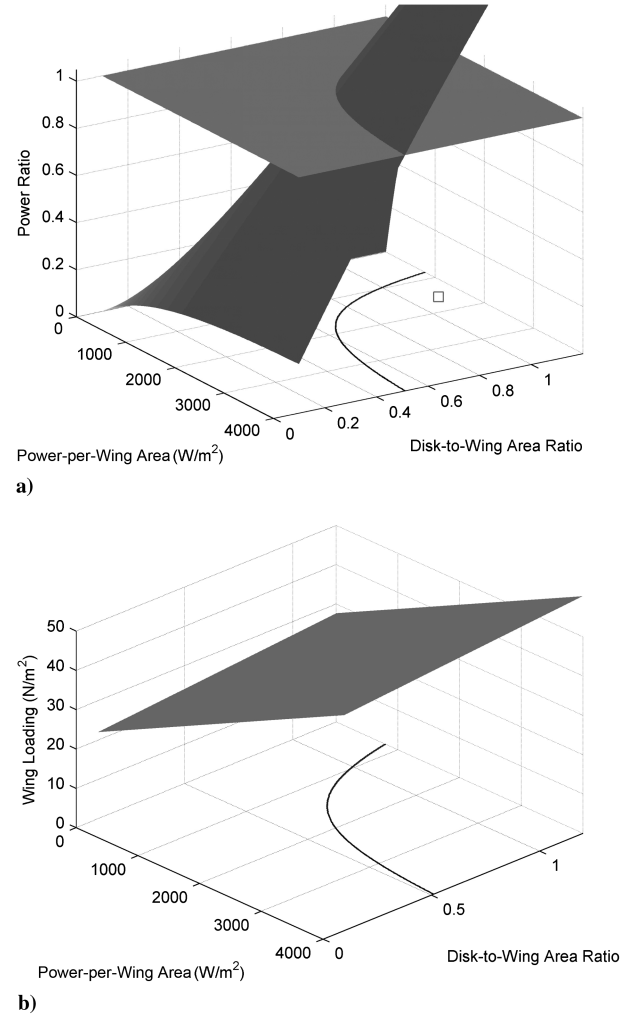
Symbols	Values	Parameters
b_w	2.42 m	Wing span
c_w	0.48 m	Mean wing chord
AR	5.11	Wing aspect ratio
S	1.15 m ²	Wing area
D_{prop}	0.636 m	Propeller diameter
n	4	Number of propellers

Table 4 Assumed parameters for sample propeller-driven Martian aircraft

Symbols	Values	Parameters
$\rho_{S,\text{wing}}$	0.572 kg/m ²	Wing surface density
h_{prop}	4 mm	Mean blade thickness
S_{prop}/A	0.3	Propeller solidity
ρ_{prop}	1797 kg/m ³	Propeller material density (carbon fiber)
$\eta_{\text{prop},E}$	0.6	Propeller efficiency on Earth
$\eta_{\text{prop},M}$	0.6	Propeller efficiency on Mars
$(A/S)_E$	0.18	Reference disk-to-wing area ratio on Earth
r_{motor}	2000 W/kg	Motor power-to-mass ratio
$E_{\text{batteries}}$	420 kJ/kg	Energy density of batteries
C_{D0}	0.0185	Zero-lift drag coefficient
e	0.8	Oswald efficiency

$P_{\text{prop},M}/S$, and the wing loading W_E/S . First, if the total weight W_E is suitably reduced, the constraints on the propeller disk area and the propulsive power would be considerably relaxed due to the power-law exponent of 3/2. Secondly, the motor power-to-mass ratio r_{motor} and propeller efficiency $\eta_{\text{prop},M}$ directly affect the propulsive power $P_{\text{prop},M}$.

The preceding procedures should be carried out iteratively in the preliminary design. Table 4 shows the assumed parameters in the design of this aircraft. In the first-round estimations, it is assumed that the surface density of the wing with a Magnesium (ZK60A) frame is $\rho_{S,\text{wing}} = W_{E,\text{wing}}/S = 0.572 \text{ kg/m}^2$. Note that a wing with a carbon fiber frame has $\rho_{S,\text{wing}} = W_{E,\text{wing}}/S = 0.343 \text{ kg/m}^2$ [27]. It is also assumed that the propeller efficiency on Earth and Mars remains the same, i.e., $\eta_{\text{prop},M} = \eta_{\text{prop},E} = 0.6$, which implies that the advance ratio coefficient remains the same in cruising flight on Earth and Mars, i.e., $J_M = J_E$. It is assumed that the four RC airplane motors (like Himax brushless DC motors) are used to drive the four propellers and the power-to-mass ratio is 2000 W/kg. Figure 10 shows the power–mass relation of Himax motors where the mean specific power is 2650 W/kg. Noth et al. [11] have collected the power data for approximately 2000 electrical motors, and found that the relation between the maximum motor power and the motor mass is approximately linear. Their regression indicates that the

**Fig. 8 The upper bound of the total weight of the sample Martian aircraft.****Fig. 9 a) The surface of Π_M intersecting with $\Pi_M = 1$, and b) the wing loading plane for the sample Martian aircraft, where the design point is indicated by a square symbol.**

power-to-weight ratio of RC airplane motors is about $r_{\text{motor}} = 3400 \text{ W/kg}$, whereas other motors including Maxon motors have $r_{\text{motor}} = 90 \text{ W/kg}$. The motor efficiency is $\eta_{\text{motor}} = 0.7\text{--}0.9$ for most motors.

The mass distribution of the aircraft is shown in Table 5. The cruising velocity is 68 m/s, and the corresponding Mach number is

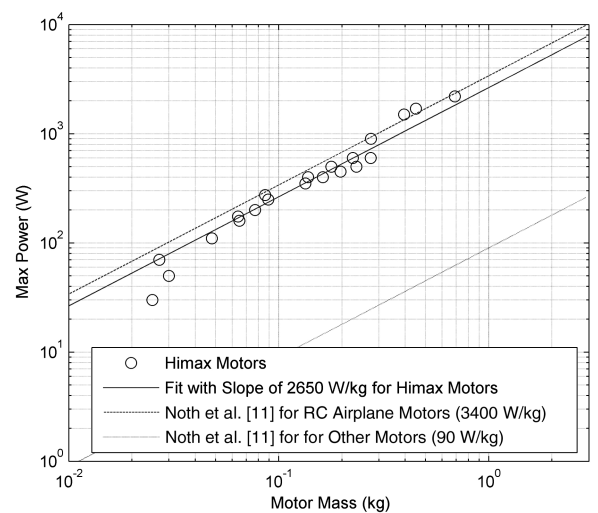
**Fig. 10 The relation between the maximum motor power and the motor mass for Himax motors and others.**

Table 5 Mass distribution of sample propeller-driven Martian aircraft

Symbols	Values	Parameters
m_E	4.24 kg	Total mass
$m_{E,\text{wing}}$	0.66 kg	Wing mass
$m_{E,\text{prop}}$	0.21 kg	Propeller mass
$m_{E,\text{motor}}$	1.50 kg	Motor mass
$m_{E,\text{others}}$	1.87 kg	Other mass

Table 6 Performance parameters of sample propeller-driven Martian aircraft

Symbols	Values	Parameters
Π_M	1.44	Power ratio on Mars
$V_{M,\text{max } R}$	68 m/s	Cruising velocity on Mars
R_M	257 km	Cruising range on Mars
E_M	1.05 h	Cruising endurance on Mars
$P_{M,\text{max } R}$	89 W	Cruising power required on Mars
$P_{\text{prop},M}$	128 W	Propulsive power available on Mars
$C_{L,M}$	0.42	Lift coefficient on Mars
W_M/S	15.3 N/m ²	Wing loading on Mars

0.23 on Mars. The Reynolds number based on the wind chord on Mars is 3.4×10^4 . The available propulsive power of 128 W on Mars is larger than the required cruising power of 89 W. The lift coefficient in cruising flight is $C_{L,M} = 0.42$, which is attainable for a wing with a suitable airfoil section. The cruising endurance and range are estimated by $E_M = E_{\text{motor}}\eta_{\text{motor}}/P_{M,\text{max } R}$ and $R_M = T_M V_{M,\text{max } R}$, respectively. The performance parameters of the aircraft are listed in Table 6. Overall, this preliminary design indicates that the sample Martian aircraft of the Japan Aerospace Exploration Agency is feasible for cruising flight on Mars. The design parameters of the sample Martian aircraft could be iteratively adjusted to meet some technological constraints.

It is noticed that an earlier design of propeller-driven aircraft the Canyon Flyer for Mars exploration was presented by NASA researchers [28]. It has a total mass of 20 kg, wing area of 0.77 m², aspect ratio of 6.3, a 1.08-m-diam propeller, and a 0.38 kg electric motor. When the other parameters are assumed to be the same as those of the sample Martian aircraft of the Japan Aerospace Exploration Agency, the estimated power ratio is $\Pi_M = 0.042 < 1$, as shown in Table 2. Therefore, the Canyon Flyer could not fly on Mars due to its high weight and low motor power.

VI. Propellers

The performance of propellers is a key for flight of Martian aircraft. For convenience of analysis, the results of the momentum blade element theory of propellers are recasted. According to McCormick [29], the thrust and power coefficients are, respectively, given by

$$K_T = \frac{T}{0.5\rho(\pi R^2)V_T^2} = \int_0^1 \sigma(\lambda^2 + x^2)C_l \cos \phi(1 - \epsilon \tan \phi) dx \quad (41)$$

$$K_P = \frac{P}{0.5\rho(\pi R^2)V_T^3} = \int_0^1 \sigma x(\lambda^2 + x^2)C_l \cos \phi(\epsilon + \tan \phi) dx \quad (42)$$

where $\sigma = Bc/\pi R$ is a solidity factor, $x = r/R$ is a normalized radial coordinate, $\lambda = V/\omega R$ is the advance ratio coefficient $\lambda = J/\pi$, $\phi = \tan^{-1}(\lambda/x)$ is the flow angle, C_l is the sectional lift coefficient, c is the blade chord, r is the radial coordinate along a blade, R is the radius of a blade, B is the number of blades, ω is the rotational speed in rad/s, and ϵ is the drag-to-lift ratio. The relations between the differently defined thrust and power coefficients are $K_T = (8/\pi^3)C_T$ and $K_P = (8/\pi^4)C_P$.

We introduce a new radial coordinate $\xi = x/\lambda$ ($\lambda \neq 0$) and then express the following term in Eqs. (41) and (42) related to the sectional lift coefficient in a Taylor expansion:

$$\sigma(\xi)\sqrt{1 + \xi^2}C_l(\xi) = \sigma_0 C_{l0} \sum_{n=0}^M a_n \xi^n \quad (43)$$

where σ_0 and C_{l0} are the reference values of σ and C_l . The blade chord distribution $c(\xi)$ is given in a design. The sectional lift coefficient $C_l(\xi)$ is determined by the circulation distribution that was modeled by Goldstein [30], Glauert [31], and Theodorsen [32]. A summary of the classical aerodynamic models of propellers is given by Wald [33]. Because $c(\xi)$ and $C_l(\xi)$ are well-behaved functions, Eq. (43) should be a good polynomial approximation. Therefore, Eqs. (41) and (42) can be expressed as

$$K_T = \sigma_0 C_{l0} \lambda^{1-M} k_1(\lambda), \quad K_P = \sigma_0 C_{l0} \lambda^{1-M} k_2(\lambda) \quad (44)$$

where

$$k_1(\lambda) = \sum_{n=0}^M \left(\frac{a_n}{n+2} \lambda^{M-n} - \epsilon \frac{a_n}{n+1} \lambda^{M-n+1} \right) \quad (45)$$

$$k_2(\lambda) = \sum_{n=0}^M \left(\frac{a_n}{n+2} \lambda^{M-n+1} + \epsilon \frac{a_n}{n+3} \lambda^{M-n} \right) \quad (46)$$

Similarly, the propeller efficiency is expressed as

$$\eta_{\text{prop}} = \lambda \frac{K_T}{K_P} = \frac{1 - \epsilon \lambda F_1(\lambda)}{1 + \epsilon \lambda^{-1} F_2(\lambda)} \quad (47)$$

where

$$F_1(\lambda) = \sum_{n=0}^M \frac{a_n}{n+1} \lambda^{M-n} / \sum_{n=0}^M \frac{a_n}{n+2} \lambda^{M-n} \quad (48)$$

$$F_2(\lambda) = \sum_{n=0}^M \frac{a_n}{n+3} \lambda^{M-n} / \sum_{n=0}^M \frac{a_n}{n+2} \lambda^{M-n} \quad (49)$$

Equation (47) explicitly shows the effect of the drag-to-lift ratio ϵ on the propeller efficiency. For fixed values of ϵ , σ_0 , and C_{l0} , the advance ratio coefficient $\lambda = J/\pi$ is the main parameter to determine the performance of a propeller. To achieve the same propeller efficiency and the thrust and power coefficients on Mars, λ should remain the same, i.e., $\lambda_M/\lambda_E = J_M/J_E = 1$. In cruising flight, based on the velocity scaling relation Eq. (4), this condition is written as

$$\frac{N_M}{N_E} = \frac{\omega_M}{\omega_E} = \left(\frac{g_M}{g_E} \right)^{1/2} \left(\frac{\rho_E}{\rho_M} \right)^{1/2} \quad (50)$$

The ratio between the rotational speeds of a propeller on the Martian surface and the sea level on Earth is $N_M/N_E = \omega_M/\omega_E \approx 5.75$, indicating that it has to spin much faster on Mars to achieve the same propeller efficiency on Earth.

Nevertheless, the potential problem of increasing the rotational speed of a propeller is that the local Mach number relative to the blade may reach or exceed the critical Mach number such that flow on the blade surface becomes transonic. In this case, the performance of the blade will be degenerated due to shock stall because the lift is decreased sharply and the drag is increased markedly [29]. It is necessary to estimate the critical rotational speed below which flow on the blade surface remains subsonic. In the first-order approximation where the interference factors due to induction of the wake vortex system are neglected, the total velocity relative to the blade is $V_R = \sqrt{\omega^2 r^2 + V^2}$ and the corresponding Mach number is

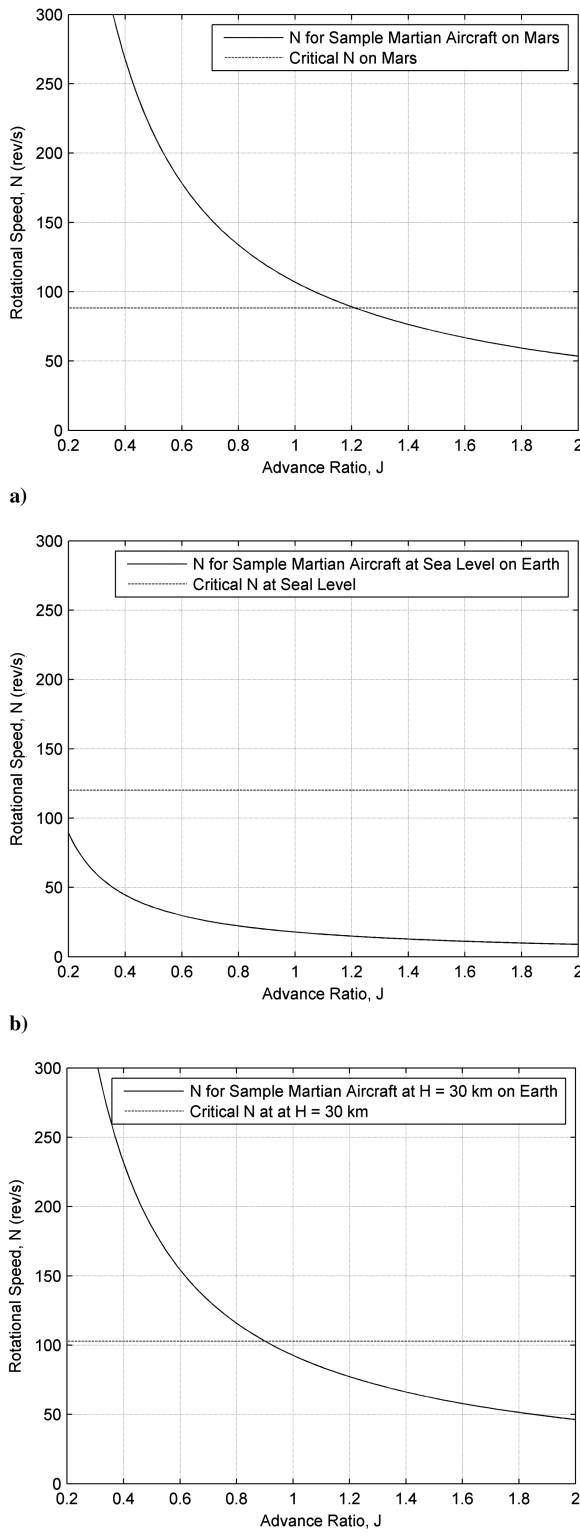


Fig. 11 Rotational speed (N) of a propeller and the critical rotational speed for the sample Martian aircraft, a) on the Martian surface, b) at the sea level on Earth, and c) at $H = 30$ km on Earth.

$M_R = V_R/a_s = M\lambda^{-1}\sqrt{x^2 + \lambda^2}$, where $M = V/a_s$ is the flight Mach number. By setting $M_R = M_{cri}$ at the blade tip $x = 1$, an estimate $\lambda_{cri} = [(M_{cri}/M)^2 - 1]^{1/2}$ is obtained for the critical advance ratio coefficient, where M_{cri} is the critical Mach number that can be determined by using the standard method for a given blade airfoil section [34]. Further, the critical rotational speed, beyond which transonic flow will occur on the blade, is given by

$$\omega_{cri} = (a_s/R)(M_{cri}^2 - M^2)^{1/2} \quad (51)$$

Then, the scaling relation for the critical rotational speeds between Mars and Earth is

$$\frac{\omega_{cri,M}}{\omega_{cri,E}} = \left(\frac{a_{s,M}}{a_{s,E}} \right) \frac{(M_{cri}^2 - M_M^2)^{1/2}}{(M_{cri}^2 - M_E^2)^{1/2}} \quad (52)$$

On the Martian surface and the sea level on Earth, $a_{s,M}/a_{s,E} = 0.782$. In general, $\omega_{cri,M}/\omega_{cri,E} < 1$. Therefore, there are the two conflicting requirements given by Eqs. (50) and (52) on the rotational speed of a propeller. The challenging task in the propeller design for a Martian aircraft is how to compensate these constraints.

To illustrate the preceding analysis of propeller, the sample Martian aircraft is considered as a typical case where the relevant parameters are listed in Tables 3–5. It is assumed that the critical Mach number for the propeller blade is $M_{cri} = 0.7$. Figure 11 shows the rotational speed N of a propeller as a function of the advance ratio coefficient J and the critical rotational speed for the sample Martian aircraft in cruising flight on the Martian surface and at the sea level and $H = 30$ km on Earth. In cruising flight on the Martian surface, as shown in Fig. 11a, N is larger than the critical rotational speed for $J < 1.18$, indicating that flow on a part of the blade surface is transonic. A similar situation can be found for the propeller at $H = 30$ km on Earth, as shown in Fig. 11c. In contrast, in the corresponding cruising flight at sea level on Earth, N is smaller than the critical one for $J > 0.2$, as shown in Fig. 11b. Therefore, a propeller of the sample Martian aircraft has to be designed to attain the high efficiency for $J > 1.2$ on Mars. It is possible to shift the peak of the propeller efficiency curve beyond $J > 1.2$ by increasing the blade angle at $r/R = 0.75$, as reported by Biermann and Hartman [35].

VII. Conclusions

The main environmental parameter that directly affects the design of propeller-driven Martian aircraft is the Martian gas density that is much lower than the air density on Earth. In addition, the gravitational constant on Mars is smaller. To take these parameters into account, the scaling relations between the performance parameters of aircraft flying on Mars and Earth are given, including the cruising velocity, power required for cruising flight, and propulsive power generated by propellers. Therefore, the performance of aircraft on Mars can be known through mapping its parameters in the Earth environment. Further, a necessary condition for cruising flight on Mars is that the ratio between the required power and the available propulsive power must be larger than one. This power ratio criterion depends on the gravitational constant ratio, the gas density ratio, and the aircraft design parameters on Earth. Several forms of this criterion are given depending on the selected parameters. Given the gravitational constant ratio and gas density ratio, the power ratio is proportional to $3/2$ -power of the motor power-to-weight ratio and the propeller efficiency. It is a function of the disk-to-wing area ratio and the propulsive power per unit wing area, and the wind loading also depends on these parameters in a linear fashion. Based on this criterion, the upper bound of the total weight of Martian aircraft is determined, which is a function of the relative motor and wing weights with a proportional factor related to the motor power-to-weight ratio and the propeller efficiency.

To validate this power ratio criterion it is applied to typical propeller-driven aircraft on Earth to predict the cruising flight ceiling and the lower bounds of the parametric domain compared with the available data. This criterion is used to examine the feasibility of the Helios Prototype in flight on Mars. The procedures of applying this criterion in the design of the sample Martian aircraft of the Japan Aerospace Exploration Agency are proposed and the preliminary data are presented. This power ratio criterion provides a necessary constraint on Martian flight. The design of propellers for Martian aircraft poses a unique challenge. The ratio between the rotational speeds of a propeller in cruising flight on Mars and Earth is given, indicating that it has to spin much faster on Mars to achieve the same

propeller efficiency on Earth. On the other hand, at a higher rotational speed, the local Mach number relative to the blade could exceed the critical Mach number such that flow on the blade becomes transonic. The critical rotational speed below which flow on the blade remain subsonic is given. The design of propellers for Martian aircraft should meet these conflicting constraints.

Acknowledgment

Tianshu Liu would like to thank the Space Science Research Division of the Japan Aerospace Exploration Agency that supported this work during the summer in 2012.

References

- [1] von Braun, W., *The Mars Project*, Univ. of Illinois Press, Urbana-Champaign, IL, 1953, pp. 9–32.
- [2] Guynn, M. D., Croom, M. A., Smith, S. C., Parks, R. W., and Gelhausen, P. A., “Evolution of a Mars Airplane Concept for the ARES Mars Scout Mission,” AIAA Paper 2003-6578, 2003.
- [3] Levine, J. S., Blaney, D. L., Connerney, J. E., Greeley, R., Head, J. E., Hoffman, J. H., Jakosky, B. M., McKay, C. P., Sotin, C., and Summer, M. E., “Science from a Mars Airplane: The Aerial Regional-Scale Environmental Survey (ARES) of Mars,” AIAA Paper 2003-6576, Sept. 2003.
- [4] Braun, R., Wright, H. S., Croom, M. A., Levine, J. S., and Spencer, D. A., “Design of the ARES Mars Airplane and Mission Architecture,” *Journal of Spaceship and Rockets*, Vol. 43, No. 5, 2006, pp. 1026–1034. doi:10.2514/1.17956
- [5] Rhew, R. D., Guynn, M. D., Yetter, J. A., Levine, J. S., and Young, L. A., “Planetary Flight Vehicles (PFV): Technology Development Plans for New Robotic Explorers,” *AIAA Infotech@Aerospace Conference*, Arlington, VA, Sept. 2005.
- [6] Colozza, A., “Comparison of Mars Aircraft Propulsion Systems,” NASA Glenn Research Center, CR-2003-212350, Cleveland, OH, 2003.
- [7] Colozza, A., “Preliminary Design of a Long-Endurance Mars Aircraft,” NASA Glenn Research Center, CR-185243, Cleveland, OH, 1990.
- [8] Colozza, A., “Solid State Aircraft,” NASA Inst. for Advanced Concepts, Atlanta, GA, Final Report, Phase II Project, NAS5-03110, 2005.
- [9] Noth, A., Engel, M. W., and Siegwart, R., “Flying Solo and Solar to Mars,” *IEEE Robotics & Automation Magazine*, Vol. 13, No. 3, Sept. 2006, pp. 44–52. doi:10.1109/MRA.2006.1678138
- [10] Noth, A., Siegwart, R., and Engel, M. W., “Autonomous Solar UAV for Sustainable Flight,” in *Advances in Unmanned Aerial Vehicles*, edited by Valavanis, K. P., Springer-Verlag, Berlin, 2007, Chap. 12.
- [11] Noth, A., and Siegwart, R., “Solar-Powered Micro-Air Vehicles and Challenges in Downscaling,” *Flying Insects and Robots*, edited by Floreano, D., Zuffery, J., Srinivasan, M., and Ellington, C., Springer-Verlag, Berlin, 2009, Chap. 20.
- [12] Klesh, A., and Kabamba, P., “Solar-Powered Unmanned Aerial Vehicles on Mars: Perpetual Endurance,” *58th International Astronautical Congress*, International Astronautical Federation, Paris, 24–28 Sept. 2007.
- [13] Lorenz, R. D., “Flight Power Scaling of Airplanes, Airships, and Helicopters: Application to Planetary Exploration,” *Journal of Aircraft*, Vol. 38, No. 2, 2001, pp. 208–214. doi:10.2514/2.2769
- [14] Savu, G., “Earth-Mars Similarity Criteria for Exploring Martian Vehicles,” *Acta Astronautica*, Vol. 59, Nos. 8–11, 2006, pp. 734–741. doi:10.1016/j.actaastro.2005.07.001
- [15] Liu, T., “Time-Area-Averaged Momentum Stream Tube Model for Flapping Flight,” *Journal of Aircraft*, Vol. 44, No. 2, 2007, pp. 459–466. doi:10.2514/1.23660
- [16] Ward, D. T., *Introduction to Flight Test Engineering*, Elsevier, Amsterdam, 1993, Chap. 4.
- [17] Kimberlin, R. D., *Flight Testing of Fixed-Wing Aircraft*, AIAA Education Series, Reston, VA, 2003, Chap. 9.
- [18] Liu, T., and Schulte, M., “Flight Testing Education at Western Michigan University,” AIAA Paper 2007-0700, 2007.
- [19] Anderson, J. D., *Aircraft Performance and Design*, McGraw-Hill, New York, 1999, Chap. 5.
- [20] Liu, T., “Comparative Scaling of Flapping- and Fixed-Wing Flyers,” *AIAA Journal*, Vol. 44, No. 1, 2006, pp. 24–33. doi:10.2514/1.4035
- [21] Adkins, C. N., and Liebeck, R. H., “Design of Optimum Propellers,” *Journal of Propulsion and Power*, Vol. 10, No. 5, 1994, pp. 676–682. doi:10.2514/3.23779
- [22] Brandt, J. B., and Selig, M. S., “Propeller Performance Data at Low Reynolds Numbers,” AIAA Paper 2011-1255, 2011.
- [23] Peigin, S., Epstein, B., Seror, S., Hoffman, G., and Dhandapani, P., “Propeller Model Development with the Accurate Navier-Stokes Solver NES,” *52nd Israel Annual Conference on Aerospace Sciences*, Technion Israel Inst. of Technology, Israel, 29–1 Feb.–March 2012.
- [24] Jackson, P., *Jane's All the World's Aircraft 2011–2012*, HIS Global Ltd., Surrey, U.K., 2011.
- [25] Noll, T. E., Ishmael, S. D., Henwood, B., Perez-Davis, M. E., Tiffany, G. C., Madura, J., Gaier, M., Brown, J. M., and Wierzbowski, T., “Technical Findings, Lessons Learned, and Recommendations Resulting from the Helios Prototype Vehicle Mishap,” In *UAV Design Processes/Design Criteria for Structures*, Meeting Proceedings RTO-MP-AVT-145, Paper 3.4, NATO Science and Technology Organization, 2007.
- [26] Oyama, A., “Multiobjective Design Exploration of Airplane for Mars Exploration,” *21st Workshop on Astrodynamics and Flight Mechanics*, Japan Aerospace Exploration Agency, Sagamihara, Kanagawa, Japan, 25 July 2011.
- [27] Yonemoto, K., “Manufacturing of Ultralight Wing,” 2012 (unpublished).
- [28] Smith, S. C., Hahn, A. S., Johnson, W. R., Kinney, D. J., Pollitt, J. A., and Reuther, J. R., “The Design of the Canyon Flyer, an Airplane for Mars Exploration,” AIAA Paper 2000-0514, 2000.
- [29] McCormick, B. W., *Aerodynamics of V/STOL Flight*, Academic Press, New York, 1967, Chap. 4.
- [30] Goldstein, S., “On the Vortex Theory of Screw Propellers,” *Proceedings of the Royal Society of London, Series A: Mathematical and Physical Sciences*, Vol. 123, No. 792, 1929, pp. 440–465. doi:10.1098/rspa.1929.0078
- [31] Glauert, H., *Airplane Propellers*, Reprinted by Dover, New York, 1963, Chap. XI.
- [32] Theodorsen, T., *Theory of Propellers*, Vol. 3, McGraw-Hill, New York, 1948.
- [33] Wald, Q. R., “The Aerodynamics of Propellers,” *Progress in Aerospace Sciences*, Vol. 42, No. 2, 2006, pp. 85–128. doi:10.1016/j.paerosci.2006.04.001
- [34] Anderson, J. D., *Fundamentals of Aerodynamics*, 5th ed., McGraw-Hill, New York, 2010, Chap. 11.
- [35] Biermann, D., and Hartman, E. P., “Tests of Five Full-Scale Propellers in the Presence of a Radial and a Liquid-Cooled Engine Nacelle, Including Tests of Two Spinners,” NACA Langley Research Center, Rept. No. 642, Hampton, VA, Nov. 1937.